Peptide-based CE-SELEX enables convenient isolation of aptamers specifically recognizing CD20-expressing cells

Jordan Cossu, Corinne Ravelet, Véronique Martel-Frachet, Eric Peyrin, Didier Boturyn

Bioorg. Med. Chem. 110 (2024) 117831

Contents lists available at ScienceDirect

Bioorganic & Medicinal Chemistry

journal homepage: www.elsevier.com/locate/bmc

Peptide-based CE-SELEX enables convenient isolation of aptamers specifically recognizing CD20-expressing cells

Jordan Cossu [a,b], Corinne Ravelet [b], Véronique Martel-Frachet [c,d], Eric Peyrin [b,*], Didier Boturyn [a,*]

[a] University Grenoble Alpes, CNRS, DCM UMR 5250, 38058 Grenoble Cedex 9, France
[b] University Grenoble Alpes, CNRS, DPM UMR 5063, 38041 Grenoble Cedex 9, France
[c] University Grenoble Alpes, IAB CNRS UMR5309, INSERM U1209, Allée des Alpes 38700, La Tronche, France
[d] University PSL Research, EPHE, 5014 Paris, France

ARTICLE INFO

Keywords:
CD20
Aptamer
SELEX
Capillary electrophoresis

ABSTRACT

The CD20 antigen is a key target for several diseases including lymphoma and autoimmune diseases. For over 20 years, several monoclonal antibodies were developed to treat CD20-related disorders. As many therapeutic proteins, their clinical use is however limited due to their nature with a costly biotechnological procedure and side effects such as the production of anti-drug neutralizing antibodies. Nucleic acid aptamers have some advantages over mAbs and are currently investigated for clinical use. We herein report the selection of DNA aptamer by using a peptide-based CE-SELEX (Capillary Electrophoresis-Systematic Evolution of Ligands by Exponential Enrichment) method. It was demonstrated that these aptamers bind specifically a CD20-expressing human cell line, with K_d estimated from isothermal titration calorimetry experiments in the micromolar range. This study demonstrates that the CE-SELEX is suitable as alternative method to the conventional Cell-SELEX to discover new cell-targeting compounds.

1. Introduction

For over 25 years, many monoclonal antibodies (mAbs) were developed to treat numerous diseases.[1] Today, they have become the main class of drugs and the best-selling in the pharmaceutical market. Among the key target of mAbs, the recognition of CD20 antigen, exclusively expressed on B cells, is used for several pathologies such as lymphoma and autoimmune diseases.[2] This antigen is the target of several mAbs including rituximab, ibritumomab, ofatumumab, obinutuzumab, and ocrelizumab. As virtually all other therapeutic proteins, administration of mAbs or their derivatives (nanobodies, mAb fragments) elicits an immune response that could lead to the production of anti-drug antibodies, acute anaphylaxis or serum sickness.[3] Additionally, their production mode requires a very expensive biotechnological procedure that involves the use of living systems, which can pose problems in terms of inter-batch variation, contamination and ethics. It is then advantageous to develop in parallel new molecular systems that integrate the benefits of mAbs while circumventing their limitations. This challenge can be met by designing antibody substitutes using a fully synthetic approach.

To this end, DNA aptamers, obtained by the SELEX (Systematic Evolution of Ligands by Exponential Enrichment) method, are increasingly investigated for clinical use because of their very low immunogenicity, their potential high affinity for their target, their structural and chemical stabilities and the fact that their production is carried out entirely by an organic synthesis process [4] avoiding for example any batch-to-batch variation. Due to their designable conformational changes, aptamers are broadly used for numerous biomedical applications such as bioanalysis, imaging and therapy.[5] To date, several RNA aptamers are currently in clinical trials or clinically used,[6] such as the aptamer pegaptanib (Macugen, Pfizer) which targets the vascular endothelial growth factor (VEGF) and was used to treat age-related macular degeneration (AMD).[7] The FDA has recently approved a prescription eye injection containing a PEGylated RNA aptamer oligonucleotide that binds to and inhibits complement protein C5 for the treatment of geographic atrophy (GA), the advanced form of dry AMD. [8]

As far as anti-CD20 aptamers are concerned, a number of functional oligonucleotides have already been identified by Cell-SELEX,[9] which is

* Corresponding authors.
E-mail addresses: eric.peyrin@univ-grenoble-alpes.fr (E. Peyrin), didier.boturyn@univ-grenoble-alpes.fr (D. Boturyn).

https://doi.org/10.1016/j.bmc.2024.117831
Received 27 May 2024; Received in revised form 4 July 2024; Accepted 4 July 2024
Available online 6 July 2024

the selection method often privileged in the case of membrane protein targets.[10] Indeed, the Cell-SELEX has key advantages such as the ability to design an aptamer against the native conformation of the proteins without the laborious process of protein purification. However, this process also has drawbacks that include interference from dead cells during selection, imperfect counter-selection, a lengthy experimental procedure and the potential of targeting unintended membrane proteins on cells.[10,11].

Herein, we report an alternative method to the Cell-SELEX that aims at facilitating the selection of DNA aptamers targeting CD20 antigen. The current approach was firstly based on the observation that the extracellular loop of the CD20 protein (amino acids N163 to Q187), constrained by a disulfide bond, contains the epitopes of most of the mAbs currently used in therapy,[12] and its interaction with the mAb rituximab was characterized using X-ray technique.[13] Recently, we reported surface plasmon resonance (SPR) studies that have shown that this CD20 fragment selectively binds rituximab with K_d values close to those reported from *in vitro* analysis with CD20-expressing cells.[14] We believed that this peculiar peptide fragment could constitute a molecular target of choice for selecting aptamers capable of recognizing CD20-expressing cells, as already achieved for certain aptamers binding to other membrane proteins.[15] In a move designed to make the whole selection process even more convenient, we opted to deploy the CE (capillary electrophoresis)-SELEX method for the aptamer identification. Using CE as a means of partitioning, nucleic acid sequences that bind to the target are separated from those that do not by a change in electrophoretic mobility. Target-binding sequences are then collected at the capillary outlet for amplification and subsequent rounding. The CE-SELEX is very practical to use for molecular targets as it requires just a few selection cycles (thanks in part to its high-resolution power) and the target does not need to be immobilized on a solid support. In 2004, Mendonsa and Bowser have reported the first CE-SELEX,[16] providing aptamers with high affinity to the IgE target (K_d below 30 nM) in only four rounds of selection. To date, more than 20 protein-binding aptamers have been isolated by this method.[17] In the case of peptide targets, the CE-SELEX is obviously trickier due to the expected smaller change in the electrophoretic mobility of DNA molecules upon target binding. However, some effective aptamers with K_d in the nanomolar range have been yet identified by implementing this partitioning technique. For instance, Bowser and co-workers have reported selection of aptamers binding the neuropeptide Y (4272 g/mol) [18] while our group has described CE-SELEX for the αC-conotoxin PrXA (3897 g/mol), an ultra-fast-killing paralytic toxin of marine snail.[19]

We performed four rounds of CE-SELEX to ensure that the DNA pool correctly evolved towards the ability to bind the above-mentioned CD-20 peptide. After NGS sequencing, we investigated the recognition properties of two candidates and some truncated variants by isothermal titration calorimetry (ITC). Finally, to illustrate the usefulness of our CD20 fragment-based CE-SELEX, *in cellulo* experiments were performed using a CD20-containing Raji cell line in comparison with a Jurkat cell line that does not express the CD20 antigen.

2. Results and discussion

2.1. Aptamer selection and optimization

All peptides, including a scrambled CD20 fragment prepared as negative control,[14a] were produced through solid phase peptide synthesis and disulfide bridge formation in solution (see Table S1, Figure S1).

As described by the Krylov lab, aptamer selection by CE-SELEX requires optimal electrophoretic separation between the target and the ssDNA library.[20] Target, unbound ssDNA and target-ssDNA complex can be separated based on their different mobilities caused by their different charge-to-mass ratio. The complex is commonly collected within the window defined between the migration times of the target and the ssDNA library. For the determination of this aptamer collection window, the peptide and the library (Table S2) were preliminary injected into the fused-silica capillary. The electrophoretic migration was carried out at 25 kV using UV detector. Both CD20 and ssDNA were shown to migrate after the neutral marker mesityl oxyde (Figure S2) and a large collection window was apparent between these two bands. To save time, the partitioning processes were then performed at 28 kV during the SELEX procedure.

After incubating 50 μM of CD20 with 30 μM of ssDNA library, the mixture was injected and the fraction in the 4–8 min window was collected (10 fractions for a round). The selection was carried out by progressively reducing the [target]/[DNA] ratio (Table S2). Between each cycle, injections of a mixture containing the target and the amplified DNA pool were used to monitor SELEX progression, showing a favorable evolution until the 4th cycle. As representative example, Fig. 1 depicts the electrophoretic profiles obtained after injection of the amplified DNA pool from the first or fourth cycle, either alone or mixed with a constant amount of CD20 peptide. For round 1, no difference in electrophoretic trace was observable between experiments with or without target (Fig. 1A and 1B). In contrast, a new band was visualized within the expected time window (at around 8 min) when the target peptide was added to the DNA pool from the fourth cycle (Fig. 1C vs. Fig. 1D), in accordance with the presence of the peptide-DNA complex. Moreover, the free DNA fraction was concomitantly diminished and quite distorted as compared with the profile observed in the absence of target. Furthermore, when using CD20-scr in place of the targeted peptide in the presence of round 4 pool, we observed an unbound DNA peak that retained its overall shape, as well as a much smaller complex peak, if any (Fig. 1E). This suggests that the interaction with the control CD20-scr was significantly weaker than that with the target. Therefore, the DNA pool obtained after 4 selection cycles appeared to display specific binding features towards the CD20 peptide and was then processed by sequencing.

More than 160,000 sequences were identified by NGS sequencing. The majority of the sequences had the expected size of 30 nucleotides for the randomized region. About 1,300 were represented 2 times and 5 were represented 3 times. The five most abundant sequences were then analyzed using the MEME-suite software in order to identify potential conserved motifs. However, no highly conserved motifs were identified, as typically observed in CE-SELEX.[21,22] Among these sequences, we have chosen two candidates (**1** and **2**) for subsequent affinity and specificity characterization by ITC.

2.2. ITC characterization of aptamers and truncated variants

As the alkaline-buffered conditions of the CE-SELEX procedure, initially used for achieving adequate electrophoretic separation of mixture components, are not usual for biological studies, ITC experiments were carried out in nearly neutral conditions (TGK buffer, pH 7.3). No interaction was found when aptamers **1** and **2** were injected into the scrambled CD20-containing cell sample (Table 1, Fig. 2, Figure S7). By contrast, when aptamers were applied to CD20 fragment, ITC measurements showed affinities in the micromolar range. Aptamers **1** and **2** recognized the peptide target with K_d of 6.4 ± 1.0 μM and 1.2 ± 0.2 μM, respectively (Table 1, Fig. 2A and 2B).

We subsequently aimed at investigating the secondary structures of aptamers **1** and **2** by using the Mfold software.[23] Predicted secondary structures are depicted in Figures S3 and S4. On the basis of this analysis, we next decided to characterize the binding properties of some truncated variants (Table S3). These were designed simply by removing the bases at the ends, which are not involved in the formation of the stem-loop structure, yielding a 51 mer (1-f1) and 36 mer (1-f2) hairpin structure for aptamer **1** (Figure S3) and a 48 mer (2-f1) hairpin structure for aptamer **2** (Figure S4). As shown for full aptamers, the three defined variants did not exhibit any interaction with the CD20-scr (Table 1). Regarding the aptamer **1-f1** (Table 1, Fig. 2D), the measured K_d (9.0 ±

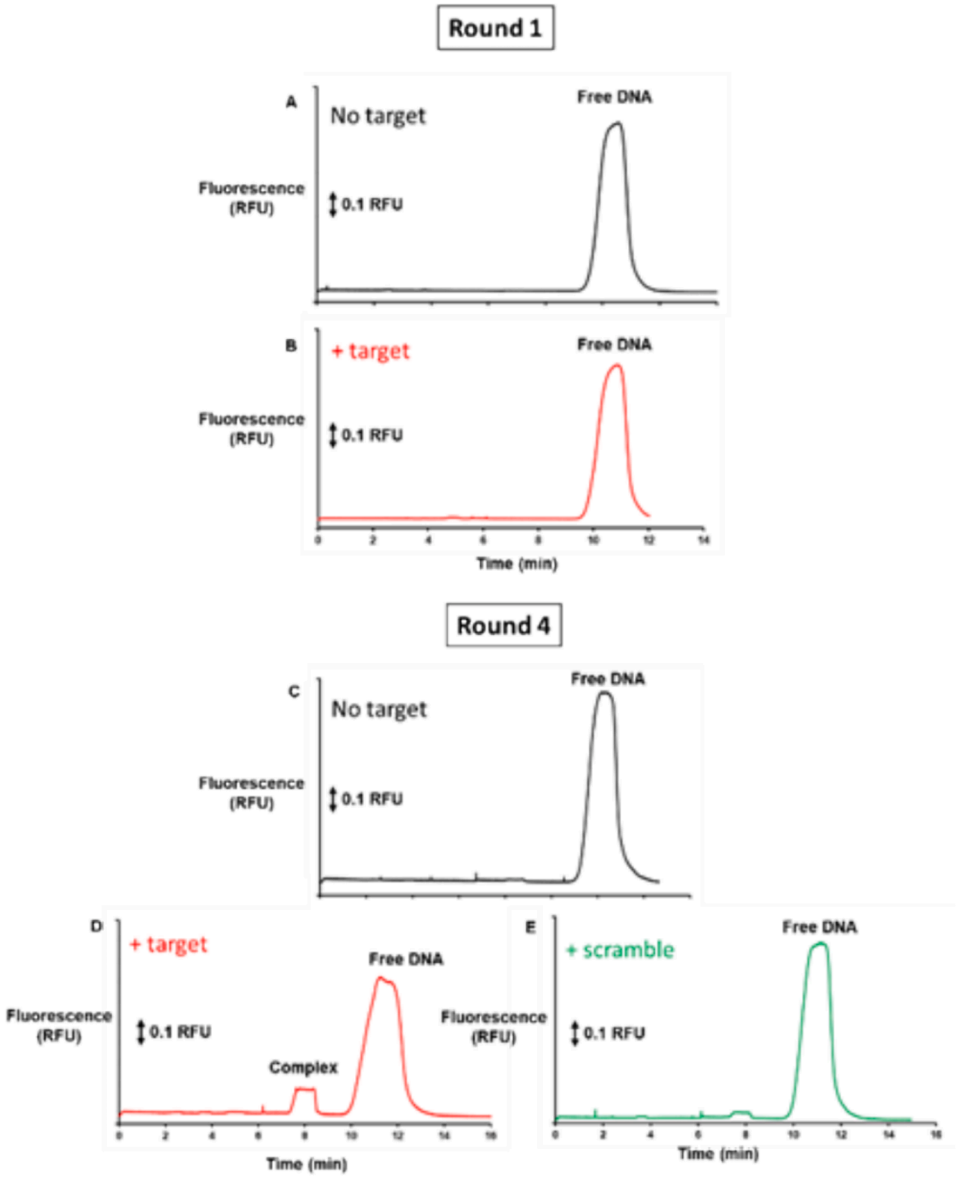

Fig. 1. Electropherograms for analysis of the amplified DNA pool from rounds 1 and 4. A) DNA pool from first round alone (10 nM); B) DNA pool from first round (10 nM) mixed with CD20 (80 μM); C) DNA pool from fourth round alone (10 nM); D) DNA pool from fourth round (10 nM) mixed with CD20 (80 μM); E) DNA pool from fourth round (10 nM) mixed with CD20-scr (80 μM). CE conditions are identical to those used during the selection process: injection: 40 s at 50 mbars; capillary total length = 72.5 cm; capillary effective length = 51.5 cm; T = 25 °C; voltage = 28 kV; TGK buffer pH 8.3.

Table 1
ITC data for aptamers interacting with CD20 or CD20 scramble obtained following injections of CD20 (2 mM) or CD20 scramble (2 mM) into a solution of aptamers (0.15 mM).

	+ CD20		+ CD20 scramble	
Aptamers	K_d (μM)	n [a]	K_d (μM)	n [a]
1	6.4 ± 1.0	0.86 ± 0.01	N/D	N/D
2	1.2 ± 0.2	1.49 ± 0.01	> mM	N/D
1-f1	9.0 ± 2.4	0.98 ± 0.02	> mM	N/D
1-f2	18.9 ± 3.3	1.07 ± 0.03	> mM	N/D
2-f1	5.5 ± 1.3	1.46 ± 0.03	> mM	N/D

[a] n is the stoichiometry of the CD20/aptamer binding.

2.4 μM) was of the same order of magnitude as found for the aptamers **1** (6.4 ± 1.0 μM) considering the error thresholds. On the contrary, a slight decrease in affinity was observed for the aptamer **1-f2** (18.9 ± 3.3 μM) and **2-f1** (5.5 ± 1.3 μM) (Table 1, Fig. 2E and 2F). It is important to note that the affinity for the aptamer **2-f1** is better than those observed for aptamer **1** fragments.

Concerning the binding stoichiometry obtained from the titration curves,[24] the data for aptamer **1** and derivatives **1-f1** and **1-f2** indicates an appropriate ratio of 1:1. The stoichiometry measured for aptamer **2** and fragment **2-f1** (n ~ 1.5) suggests an unexpected formation of complexes that could be composed of two aptamers and three CD20. While most aptamers generally bind to one target molecule, multiple binding has already been described in the literature, for example for the adenosine binding.[25]

2.3. Biological evaluation

To better evaluate the specificity of our aptamers, we next performed biological experiments using the CD20-expressing Raji cell line that origins from human Burkitt lymphoma and the CD20-free Jurkat cell line derived from human T lymphocyte cells (Figure S5). The binding affinity was assessed by flow cytometry using cyanine 5-labelled

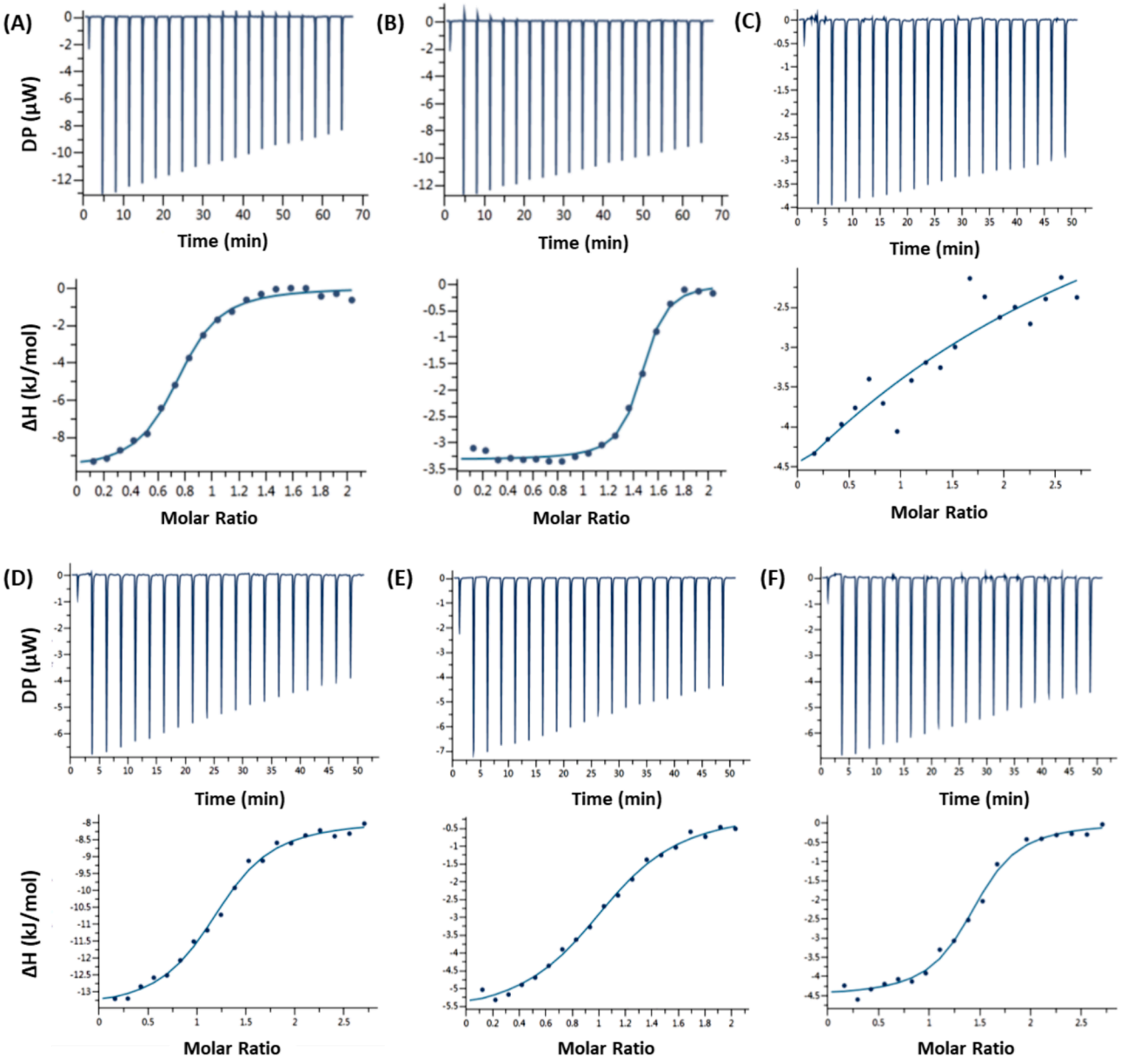

Fig. 2. Thermograms and corresponding titration curves obtained by injections of CD20 (2 mM) in solutions of (A) aptamer **1** (0.15 mM), (B) aptamer **2** (0.15 mM), (D) aptamer **1-f1** (0.15 mM), (E) aptamer **1-f2** (0.15 mM), (F) aptamer **2-f1** (0.15 mM), and by injection of CD20 scramble (2 mM) in a solution of (C) aptamer **2** (0.15 mM).

aptamers. We first investigated whether the specificity was influenced by the aptamer concentration. Both cell lines were incubated with aptamer **1** at concentrations varying from 0.5 µM to 10 µM at 25 °C. As expected, the mean fluorescence for the Raji cell line increased with the concentration while weaker fluorescence signals were observed for the control Jurkat cell line even at high concentrations (Figure S6). The ratios of labeled cells to unlabeled cells gradually increases for Raji from ~ 40 at 0.5 µM to 935 at 10 µM of aptamer **1**. On the contrary, ratios for Jurkat cells increase only slightly (3.5 at 0.5 µM to 67 at 10 µM of aptamer **1**) in favor of non-specific binding. Nevertheless, non-specific binding is significant above 2 µM of aptamer **1**. It is important to note that autofluorescence of Jurkak is much higher than for Raji cells. Additionally, we observed that the percentage of Raji unlabeled cells is very low even at submicromolar concentrations (less than 5 %). Considering these results and significant non-specific binding of aptamer **1** on Jurkat cells at concentrations above 2 µM, we then compared the efficiency of aptamers **1** and **2** for the cell binding at low concentrations (Fig. 3). Non-specific binding to Jurkat cells was observed but it is less pronounced for aptamer **1** than for aptamer **2**. By contrast, a clear increase of fluorescence was observed when aptamer **1** was added to Raji cells. At 1 µM and 0.5 µM aptamer **1**, we measured respectively an increase of 3 and 2 for the binding to Raji cells compared to Jurkat cells. In contrast, for aptamer **2** the difference between Raji and Jurkat cells is less pronounced. Considering the ITC experiments and the high binding stoichiometry for aptamer **2**, it was unsurprising that the CD20 interaction at the cell surface is less favorable than using the aptamer **1** showing an expected binding stoichiometry (n ~ 1). The biological assays concerning the aptamer **1** is in total agreement with ITC experiments.

In order to characterize the specificity of the aptamer variants, flow cytometry experiments were performed with aptamers **1-f1**, **1-f2** and **2-f1** at 0.5 µM at 25 °C (Fig. 4). For all truncated aptamers, the diminution in fluorescence intensity seems to correlate with the decrease in sequence length, while the non-specific binding does not decrease as

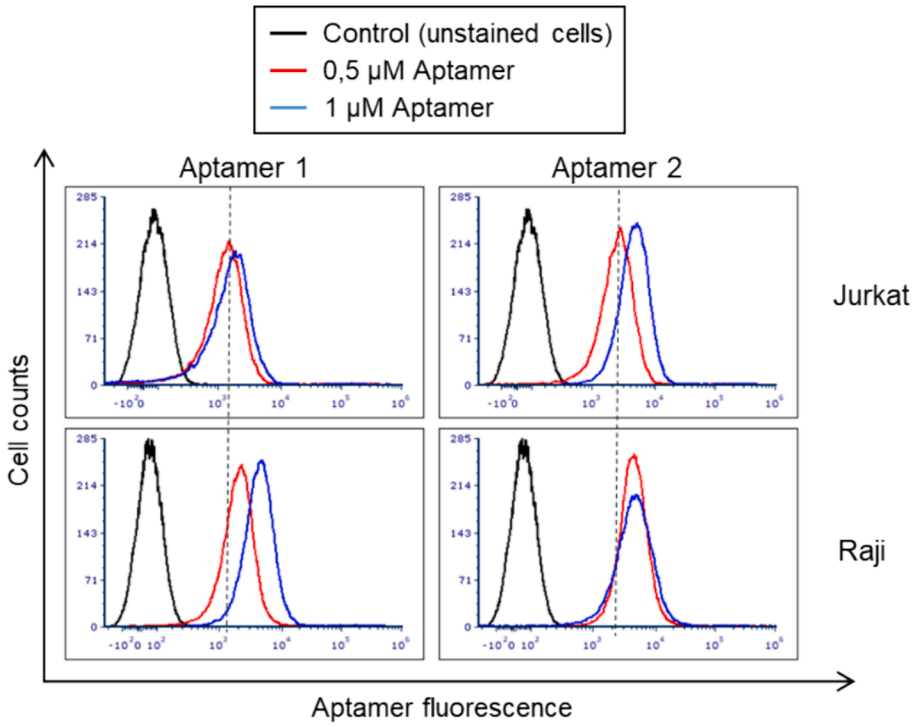

Fig. 3. Evaluation of the binding affinity of aptamers **1** and **2**. Cells (5 x 10^5 /sample) were incubated with aptamers at 25 °C in PBS for 15 min. Data representative of 2 independent experiments.

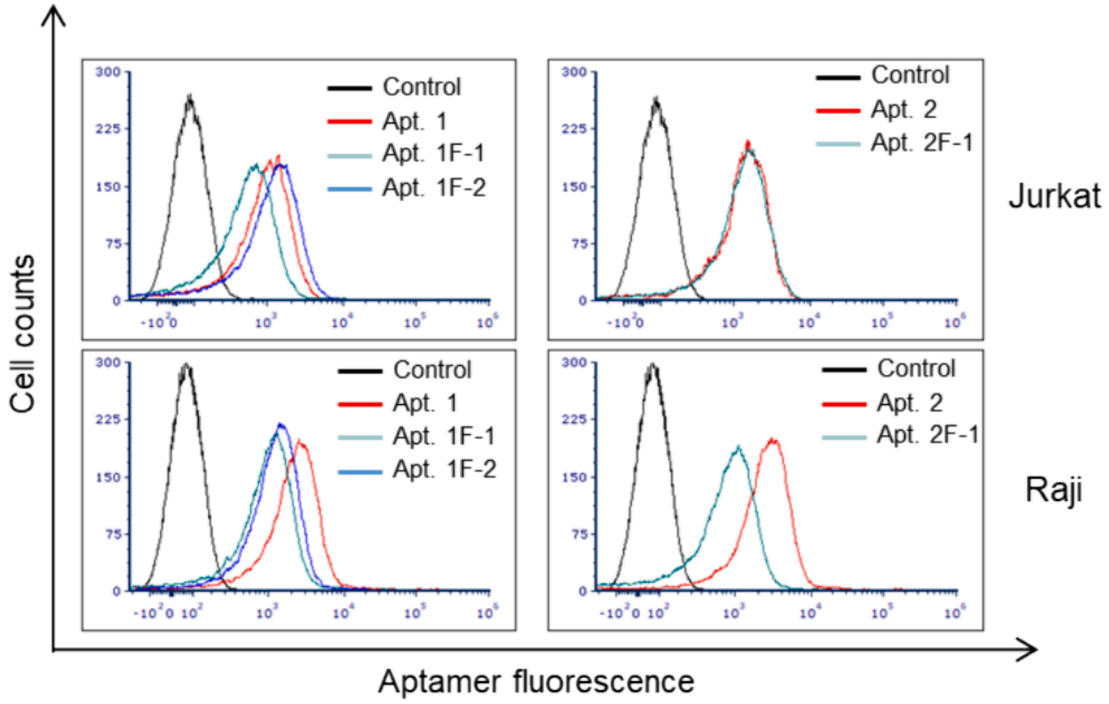

Fig. 4. Evaluation of the binding affinity of truncated aptamers. Cells (5 x 10^5 /sample) were incubated with aptamers (0.5 µM) at 25 °C in PBS for 15 min. Data representative of 3 independent experiments.

much except for aptamer **1-f1**. These results indicate the importance of nucleic acid bases not involved in the stem-loop structures. They are also consistent with ITC values (Fig. 2, Table 1).

Few studies have reported the selection of anti-CD20 aptamers by using only the Cell-SELEX technique.[9] A commercially CD20-transfected cell line is commonly used for the selection. Other process using lymphoma does not guarantee the selection of anti-CD20 aptamers.[26] To date, high molecular weight DNA aptamers (88–100 base lengths) with apparent submicromolar K_d were selected and used to study anti-CD20 antibody responses [9a] and cell tracking.[9b] As previously mentioned, there are significant disadvantages to the Cell-SELEX technique that comes from a lengthy delicate biological procedure including

interference from dead cells throughout the selection, defective counter-selection, and the possible targeting of undesired membrane proteins on cells.[10,11] In our study, for the first time DNA aptamers were obtained from the CE-SELEX after only four rounds of selection using a small peptide target (25 amino acids).

In this context, aptamers **1** was shown to be selective for the human B lymphoblastoid Raji cell line with moderate affinity in the micromolar range. Moreover, the potential limitations of typical aptamers vs. antibody include reduced *in vivo* retention times but also the lack of a multivalent association. As demonstrated earlier, the design of multivalent ligands generally provides enhanced affinities and improved biological effects.[27] For instance, trimeric and tetrameric DNA aptamer constructs were shown to exhibit high avidity at physiological temperatures both *in vitro* and *in vivo*.[28] Interestingly, it has been shown that an anti-CD20 DNA aptamer-polymer conjugate is able to induce apoptosis in targeting lymphoma cells *via* the crosslink of CD20 epitope.[29] It will be interesting to study the influence of multivalency on the binding affinity of Aptamer **1** and its fragment **1-f1** that provides less non-specific binding to CD20-expressing cells. To produce multimeric aptamers in a controlled presentation, the use of a molecular scaffold may be considered.[30]

3. Conclusion

Nucleic acids including aptamers own suitable properties for a clinical use and could be used in addition to classical pharmaceutical drugs. In this study, we were interested in the targeting of the CD20 antigen that remains a key target for numerous immunotherapies. Among methods used to discover new nucleic acid ligands, we selected the CE-SELEX as it is a convenient and a fast technique. Anti-CD20 DNA aptamers were then selected and characterized by ITC experiments. Among selected aptamers, the aptamer **1** was found to be selective for relevant CD20-expressing Raji cells although it binds CD20 with moderate affinity. In this context, the design of multimeric aptamer conjugates will pave the way to discover efficient compounds mimicking the dimeric antibody recognition. Alternatively, it will be interesting to evaluate new nucleic acid libraries with modified bases to increase interactions between the CD20 target and bank sequences, and/or to improve stability of aptamers. We recognize the significant challenge posed by using a short peptide target. Nevertheless, this work highlights the CE-SELEX as a suitable method to discover new cell-targeting compounds.

4. Materials & methods

4.1. Synthesis of CD20 peptides

Assembly of all protected peptides was carried out using the Fmoc/*t*-Bu strategy automatically on a peptide synthesizer using 2-chlorotritylchloride®. Coupling reactions were performed manually by using 2 eq. of *N*-Fmoc-protected amino acid (relative to the resin loading) activated *in situ* with 2 eq. of PyBOP and 3–5 eq. of diisopropylethylamine (DIPEA) in DMF (10 mL/g resin) for 30 min. *N*-Fmoc protecting groups were removed by treatment with a piperidine/DMF solution (1:4) for 10 min (10 mL/g resin). The process was repeated three times and the deprotection was verified by reading the absorbance of the piperidine washings at 299 nm. The linear peptides were then released from the resin by treatments with a solution containing TFA/H_2O/TIS (95/2.5/2.5, v/v/v) 3 times for 10 min. After evaporation, diethyl ether was added to precipitate peptides. Then they were triturated and washed three times with diethyl ether to obtain crude materials. Disulfide bridge formation of peptides (500 μM) was performed under mild oxidative conditions (0.1 M TrisBase, 5 % DMSO, 20 mM guanidine) during 24 h. Peptides were then purified by Reverse-Phased High-Pressure Liquid Chromatography (RP-HPLC) using a Nucelosil® C18 column (250 × 21 mm) under a 10–60 % acetonitrile linear gradient containing 0.1 % TFA. Peptides were characterized by using electron spray ionization mass technique on an Esquire 3000 spectrometer (Bruker).

4.2. Aptamer selection against the CD20 fragment

CE-SELEX was performed using a 77-nucleotide single-stranded DNA (ssDNA) library containing a randomized region of 30-nt central region flanked by two conserved primer hybridization regions (24-nt at 5′ end position (5′-FAM-GCCTGTTGTGAGCCTCCTGTCGAA)) and 23-nt at 3′ end position (TTGAGCGTTTATTCTTGTCTCCC-3′)). All oligonucleotides used for PCR amplification are shown in Table S1. The selection was performed on an Agilent 7100 Capillary Electrophoresis system (Santa Clara, California, USA) with exchangeable UV absorbance (λ 210 nm) and Picometrics ZETALIFTM LED (λ_{exc} 480 nm) Detector. For fluorescent detection, the capillary was 72.5 cm long with an effective length of 51.5 cm between the inlet and the fluorescent detection window. For UV analysis, the total length of the capillary was 60 cm with the same effective length of 51.5 cm. The fused-silica capillaries had an inner diameter of 75 μm and an outer diameter of 360 μm (Polymicro Technologies Inc., Phoenix, Arizona, USA).

The capillaries were conditioned by performing the following washes at 1 bar: 1 M NaOH for 10 min, water for 5 min and TGK buffer (25 mM Tris, 192 mM Glycine, 5 mM KH_2PO_4; pH 8.3) for 30 min. The washing process between runs was performed at 1 bar with 1 M NaOH (5 min), water (2 min) and TGK buffer (5 min). DNA library was heated at 80 °C for 10 min and left at room temperature for 20 min. For each selection round, DNA sequences, target peptide and TGK buffer were combined in 50 μL total volume. The mixture was incubated at room temperature for 40 min. For the first round of selection, the library was used with 30 μM concentration in the incubated sample. Subsequent rounds of selection used collected DNA, amplified and purified from the previous round as the input DNA. Input DNA concentrations were 166 nM, 1 μM and 1 μM for rounds 2, 3 and 4 respectively. Approximately 10^{13} sequences were introduced into the capillary in the first round of selection. Peptide concentrations were 1 μM for the first round and 500 nM, 300 nM and 30 nM for rounds 2, 3 and 4, respectively (Table S2). The equilibrated sample was injected at 50 mbar for 40 s and separated under a 28 kV voltage. UV detection was used to monitor the separation. During a selection round, the eluate corresponding to the bound DNA peak was collected into 100 μL TGK buffer. The injection, separation and collection process were repeated 10 times for each round.

The progress of the selection as well as the binding ability of sequenced candidates was monitored using CE, as previously described.[22] The experimental conditions (length capillary, preconditioning, migration buffer, voltage, temperature) were identical to those used for the CE-SELEX, except for sample preparation. Each sample contained 10 nM of enriched DNA pools and CD20 or CD20-scr was added to a concentration of 50 μM.

4.3. PCR amplification and single-stranded DNA production

Single-stranded DNA candidates were generated using a 5′-phosphate-reverse primer and a 5′-FAM-labeled forward primer during each round of the selection procedure. Subsequently, the PCR product was purified on a Nanosep® Centrifugal Device with Omega™(modified polyethersulfone) 10 K Membrane (Pall, Washington, New York, USA), and then decomposed into single-stranded DNA by lambda-exonuclease catalysis (New England Biolabs, Ipswich, MA, USA). PCR were performed using a Biometra cycler from Labgene (Archamps, France). Master mix was made by combining 668.8 μL nuclease-free water, 35.2 μL dNTPs (6.25 mM of each) (Invitrogen, Cergy Pontoise, France), 11 μL each of 5′-FAM-forward and reverse primers (10^{-4} M), 88 μL $MgCl_2$ (25 mM), 110 μL of GeneAmp 10X PCR buffer II (500 mM potassium chloride and 100 mM Tris-HCl, pH 8.3) and 5 % (v/v) of DMSO. After mixing, 11 μL (5 U/μL) of AmpliTaq Diamond DNA polymerase was

added. To finish, around 110 µL of DNA collected during selection were added. This mixed solution was divided equally over thin-walled tubes (100 µL) that were subjected to PCR. The thermal cycling regime was: initial denaturation for 3 min at 95 °C, and then cycling for 60 s at 95 °C, 60 s at 60 °C and 90 s at 72 °C for 20 cycles. After a Nanosep 10 K purification, the samples, which contained different amounts of amplified products, were combined and then decomposed into single-stranded DNA by lambda-exonuclease (5U/µL) catalysis. The filtrate was removed using the Monarch® PCR clean up kit (New England Biolabs T1030S) according to the manufacturer's protocol and quantified by absorbance at 260 nm on a Shimadzu UV mini-1240 spectrophotometer with a Tray Cell from Hellma Analytics (Müllheim, Germany). The enriched library from round 4 was processed by illumina sequencing realized by Biofidal (Vaulx en Velin, France).

4.4. ITC measurements

ITC experiments were performed with a MicroCal PEAQ-ITC isothermal titration calorimeter from Malvern (Palaiseau, France) and the data were analyzed using the software Origin (Microcal Analysis Origin Launcher). Aptamers and targets were dissolved in TGK Buffer (see previous section for binding buffer composition) at pH 7.4. Experiments were carried out in a microcalorimeter cell (300 µL) containing the aptamers (150 µM) at 25 °C. A total of 19 injections of 2 µL of sCD20 or sCD20 scramble (2 mM) were performed. At least two independent titrations were run. The experimental data were fitted to a theoretical titration curve using the Microcal PEAQ-ITC analysis software, with ΔH (enthalpy change), K_a (association constant), and N (number of binding sites per monomer) as adjustable parameters. Dissociation constant (K_d), free energy change (ΔG), and entropy contributions (TΔS) were derived from the equation $\Delta G = \Delta H - T\Delta S = -RT\cdot\ln(K_a)$ (where T is the absolute temperature and $R = 8.314\ J\cdot mol^{-1}\cdot K^{-1}$ and $K_a = 1/K_d$). Two or three independent titrations were performed for each ligand.

4.5. Biological evaluation

Cell lines, Raji (Burkitt's lymphoma) and Jurkat (T lymphocyte) were purchased from the American Type Culture Collection. All cells were cultured in RPMI 1640 medium supplemented with 10 % fetal bovine serum (heat-inactivated; Invitrogen). Flow cytometry experiment were conducted on a Attune NxT cytometer from ThermoFisher. Excitation was set at 633 nm, and emission was collected with a 670/14 bandpass filters for the Cyanine 5-tagged oligonucleotides. The data were then treated using the FSC Express 7 software.

All *in vitro* experiments were done using either RPMI 1640 or PBS buffers (ThermoFisher) as binding buffer and as washing buffer. Affinity of each construct was evaluated by incubating Raji or Jurkat cells ($5x10^5$ cells) with a series of Cyanine 5-labelled aptamers in a 50 µL of binding buffer at 25 °C for 15 min. Cells were then washed with 200 µL of washing buffer and resuspended in 200 µL of washing buffer. The binding of the aptamer was analyzed using flow cytometry by counting 20 000 events. As a positive control, a similar assay was performed using an Alexa 488-labeled anti-CD20 antibody (Biolegend).

CRediT authorship contribution statement

Jordan Cossu: Investigation. **Corinne Ravelet:** Writing – original draft, Validation, Supervision, Methodology, Formal analysis. **Véronique Martel-Frachet:** Writing – original draft, Validation, Supervision, Methodology. **Eric Peyrin:** Writing – review & editing, Writing – original draft, Validation, Supervision, Project administration, Methodology, Funding acquisition. **Didier Boturyn:** Writing – review & editing, Writing – original draft, Validation, Supervision, Project administration, Methodology, Funding acquisition, Formal analysis, Conceptualization.

Declaration of competing interest

The authors declare that they have no known competing financial interests or personal relationships that could have appeared to influence the work reported in this paper.

Data availability

Data will be made available on request.

Acknowledgements

This work was supported by the CNRS, the University Grenoble Alpes and the LabEx ARCANE and CBH-EUR-GS (ANR-17-EURE-0003). Jordan Cossu acknowledges the LabEx ARCANE for his PhD grant support, and Dr Farid Oukacine for his advice on Taylor Dispersion Analysis.

Appendix A. Supplementary material

Supplementary data to this article can be found online at https://doi.org/10.1016/j.bmc.2024.117831.

References

1. Ecker DM, Dana Jones S, Levine HL. The therapeutic monoclonal antibody market. *Mabs*. 2015;7:9–14.
2. Hofmann K, Clauder A-K, Manz RA. Targeting B cells and plasma cells in autoimmune diseases. *Front Immunol*. 2018;9:835.
3. Hansel TT, Kropshofer H, Singer T, Mitchell JA, George AJT. The safety and side effects of monoclonal antibodies. *Nat Rev Drug Discov*. 2010;9:325–328.
4. Wang T, Chen C, Larcher LM, Barrero RA, Veedu RN. Three decades of nucleic acid aptamer technologies: lessons learned, progress and opportunities on aptamer development. *Biotech Adv*. 2019;37:28–50.
5. a) Meng H-M, Liu H, Kuai H, Peng R, Mo L, Zhang X-B. Aptamer-integrated DNA nanostructures for biosensing, bioimaging and cancer therapy. *Chem Soc Rev*. 2016;45:2583–2602.b) Zhang H, Zhou L, Zhu Z, Yang C. Recent progress in aptamer-based functional probes for bioanalysis and biomedicine. *Chem Eur J*. 2016;22:9886–9900.c) Zhu G, Chen X. Aptamer-based targeted therapy. *Adv Drug Deliv Rev*. 2018;134:65–78.
6. Ni S, Zhuo Z, Pan Y, et al. Recent progress in aptamer discoveries and modifications for therapeutic applications. *ACS Appl Mater Interfaces*. 2021;13:9500–9519.
7. Ng EW, Shima DT, Calias P, Cunningham EJ, Guyer DR, Adamis AP. Pegaptanib, a targeted anti-VEGF aptamer for ocular vascular disease. *Nat. Rev. Drug Discov.* 2006;5:123–132.
8. see https://izervay.com/.
9. a) Al-Youssef NL, Ghobadloo SM, Berezovski MV. Inhibition of complement dependent cytotoxicity by anti-CD20 aptamers. *RSC Adv*. 2016;6:12435–12438.b) Haghighi M, Khanahmad H, Palizban A. Selection and characterization of single-stranded DNA aptamers binding human B-Cell surface protein CD20 by cell-SELEX. *Molecules*. 2018;23:715.
10. Rosch JC, Neal EH, Balikov DA, Rahim M, Lippmann ES. CRISPR-mediated isogenic cell-SELEX approach for generating highly specific aptamers against native membrane proteins. *Cell Mol Bioeng*. 2020;13:559–574.
11. Bakhtiari H, Ali Palizban A, Khanahmad H, Reza MM. Novel approach to overcome defects of cell-SELEX in developing aptamers against aspartate β-hydroxylase. *ACS Omega*. 2021;6:11005–11014.
12. Klein C, Lammens A, Schäfer W, et al. Epitope interactions of monoclonal antibodies targeting CD20 and their relationship to functional properties. *MAbs*. 2013;5:22–33.
13. a) Du J, Wang H, Zhong C, et al. Structural basis for recognition of CD20 by therapeutic antibody rituximab. *J Biol Chem*. 2007;282:15073–15080.b) Rougé L, Chiang N, Steffek M, et al. Structure of CD20 in complex with the therapeutic monoclonal antibody rituximab. *Science*. 2020;367:1224–1230.c) Kumar A, Planchais C, Fronzes R, Mouquet H, Reyes N. Binding mechanisms of therapeutic antibodies to human CD20. *Science*. 2020;369:793–799.
14. a) Bar L, Dejeu J, Lartia R, et al. Impact of antigen density on recognition by monoclonal antibodies. *Anal Chem*. 2020;92:5396–5403.b) Bar L, Nguyen C, Galibert M, et al. Determination of the rituximab binding site to the CD20 epitope using SPOT synthesis and surface plasmon resonance analyses. *Anal Chem*. 2021;93:6865–6872.
15. a) Janas T, Janas T. The selection of aptamers specific for membrane molecular targets. *Cell Mol Biol Lett*. 2011;16:25–39.b) Liu Z, Duan JH, Song YM, et al. Novel HER2 aptamer selectively delivers cytotoxic drug to HER2-positive breast cancer cells in vitro. *J Transl Med*. 2012;10:148.c) Hu Y, Duan J, Cao B, et al. Selection of a novel DNA thioaptamer against HER2 structure. *Clin. Transl. Oncol.* 2015;17:647–656.
16. Mendonsa SD, Bowser MT. In vitro evolution of functional DNA using capillary electrophoresis. *J Am Chem Soc*. 2004;126:20–21.

17. Zhu C, Yang G, Ghulam M, Li L, Qu F. Evolution of multi-functional capillary electrophoresis for high-efficiency selection of aptamers. *Biotechnol Adv*. 2019;37, 107432.
18. Mendonsa SD, Bowser MT. In vitro selection of aptamers with affinity for neuropeptide Y using capillary electrophoresis. *J Am Chem Soc*. 2005;127: 9382–9383.
19. Abd El-Aziz TM, Ravelet C, Molgo J, et al. Efficient functional neutralization of lethal peptide toxins in vivo by oligonucleotides. *Sci Rep*. 2017;7:7202.
20. Berezovski MV, Musheev MU, Drabovich AP, Jitkova JV, Krylov SN. Non-SELEX: selection of aptamers without intermediate amplification of candidate oligonucleotides. *Nat Protoc*. 2006;1:1359–1369.
21. Jing M, Bowser MT. Tracking the emergence of high affinity aptamers for rhVEGF165 during capillary electrophoresis-systematic evolution of ligands by exponential enrichment using high throughput sequencing. *Anal Chem*. 2013;85: 10761–10770.
22. Lisi S, Fiore E, Scarano S, et al. Non-SELEX isolation of DNA aptamers for the homogeneous-phase fluorescence anisotropy sensing of tau Proteins. *Anal Chim Acta*. 2018;1038:173–181.
23. Zuker M. Mfold web server for nucleic acid folding and hybridization prediction. *Nucleic Acids Res*. 2003;31:3406–3415.
24. Sakamoto T, Ennifar E, Nakamura Y. Thermodynamic study of aptamers binding to their target proteins. *Biochimie*. 2018;145:91–97.
25. Zhang Z, Oni O, Liu J. New insights into a classic aptamer: binding sites, cooperativity and more sensitive adenosine detection. *Nucleic Acids Res*. 2017;45: 7593–7601.
26. Tang Z, Shangguan D, Wang K, et al. Selection of aptamers for molecular recognition and characterization of cancer cells. *Anal Chem*. 2007;79:4900–4907.
27. a) Mammen M, Choi S-K, Whitesides GM. Polyvalent interactions in biological systems: implications for design and use of multivalent ligands and inhibitors. *Angew Chem Int Ed*. 1998;37:2754–2794.b) Joshi A, Vance D, Rai P, Thiyagarajan A, Kane RS. The design of polyvalent therapeutics. *Chem Eur J*. 2008;14:7738–7747.
28. Mallikaratchy PR, Ruggiero A, Gardner JR, et al. A multivalent DNA aptamer specific for the B-cell receptor on human lymphoma and leukemia. *Nucl Acids Res*. 2011;39:2458–2469.
29. Wu C, Wan W, Zhu J, Jin H, Zhao T, Li H. Induction of potent apoptosis by an anti-CD20 aptamer via the crosslink of membrane CD20 on non-Hodgkin's lymphoma cells. *RSC Adv*. 2017;7:5158–5166.
30. Cossu J, Thoreau F, Boturyn D. Multimeric RGD-based strategies for selective drug delivery to tumor tissues. *Pharmaceutics*. 2023;15:525.